

Structures and vibrations of phenol(NH₃)₂₋₄ clusters

M. Schmitt, Ch. Jacoby, M. Gerhards, C. Unterberg, W. Roth et al.

Citation: *J. Chem. Phys.* **113**, 2995 (2000); doi: 10.1063/1.1286916

View online: <http://dx.doi.org/10.1063/1.1286916>

View Table of Contents: <http://jcp.aip.org/resource/1/JCPSA6/v113/i8>

Published by the [American Institute of Physics](#).

Additional information on *J. Chem. Phys.*

Journal Homepage: <http://jcp.aip.org/>

Journal Information: http://jcp.aip.org/about/about_the_journal

Top downloads: http://jcp.aip.org/features/most_downloaded

Information for Authors: <http://jcp.aip.org/authors>

ADVERTISEMENT



AIPAdvances

Special Topic Section:
PHYSICS OF CANCER

Why cancer? Why physics? [View Articles Now](#)

Structures and vibrations of phenol(NH₃)_{2–4} clusters

M. Schmitt,^{a),b)} Ch. Jacoby, M. Gerhards, C. Unterberg, W. Roth,^{c)} and K. Kleinermanns^{a)}
*Institut für Physikalische Chemie und Elektrochemie I, Heinrich-Heine-Universität Düsseldorf,
40225 Düsseldorf, Germany*

(Received 21 December 1999; accepted 22 May 2000)

Vibronic spectra of PhOH(NH₃)_n clusters with $n=2-4$ have been obtained by resonant two-photon ionization, recorded at the mass channels of the fragment ions (NH₃)_nH⁺. The PhOH(NH₃)_{2–4} spectra show long progressions of at least one low frequency vibration pointing to different S_0 and S_1 geometries along this coordinate. In addition, the vibronic bands of the $n=2$ cluster are split into two components. A tunneling motion is discussed, which may be responsible for these splittings. To get more information about the structure of PhOH(NH₃)₂ in the electronic ground state, IR–UV double resonance spectroscopy has been applied. Possible geometries for the $n=2-4$ clusters are considered based on a comparison between the experimental data and theoretical results from *ab initio* calculations, performed at the Hartree–Fock and second-order Møller–Plesset perturbation theory level. © 2000 American Institute of Physics. [S0021-9606(00)00132-X]

I. INTRODUCTION

Hydrogen bonds with O–H···N bridges are very important in chemistry and biology. A prototype of O–H···N hydrogen bonded clusters is the PhOH(NH₃)_n system, which can be studied to obtain a detailed picture of processes like proton transfer and acid-base reactions, in different electronic states and in the ion.

The simplest aromatic O–H···N hydrogen bonded cluster is the binary PhOH(NH₃)₁, which has been investigated both experimentally and theoretically by several groups.^{1–10} In a previous publication⁶ we identified several intermolecular vibronic bands of the 1:1-cluster by two-color resonant two-photon ionization (R2PI) spectroscopy and spectral hole burning (SHB). The remaining R2PI signals on the mass channel of the $n=1$ cluster were proved to be due to fragmentation of higher clusters.⁶ For the $n=2$ cluster, several bands were observed in the one-color R2PI spectrum,² which are redshifted to the electronic origin of the binary cluster.

In the following we show that the spectrum of the PhOH(NH₃)₂ cluster can be improved considerably compared to previous publications^{2,6} by dissociative proton transfer (dPT) spectroscopy,¹¹ which utilizes the fact that the clusters show strong fragmentation to (NH₃)_nH⁺ after two-photon excitation but little evaporation of ammonia as competing channel. For the first time we are able to record vibronic spectra of the $n=3$ and 4 clusters using this product yield as signal. We assume that proton transfer takes place in the cluster ions, at least at the large excess energies under the one-color two-photon conditions in our experiments. Proton transfer has already been observed for PhOH(NH₃)₁ by trapped ion photodissociation spectroscopy of the phenoxy radical in PhO···(NH₄)⁺.¹² Kim *et al.* performed a guided-ion beam experiment between vibrationally state se-

lected phenol⁺ ions and ND₃¹³ to investigate the proton transfer in phenol(NH₃)₁⁺. In contrast to the work of Mikami, Sato, and Ishigaki¹² they found that there is no significant barrier to PT on the ionic surface. The proton affinity of ammonia increases considerably with cluster size.¹⁴ In combination with the large excess energy from one-color ionization this leads to proton transfer and fragmentation of PhOH(NH₃)_{n>1}⁺. In a very recent communication, Pino *et al.*¹⁵ showed that under two-color conditions a competing channel for proton transfer in the $n=3$ cluster is the hydrogen atom transfer in the S_1 state. This hydrogen atom transfer is followed by dissociation to the phenoxy radical and (NH₄)(NH₃)₂, which is subsequently ionized by the second color. In future experiments the branching ratio between the two competing channels has to be determined as a function of cluster size and excess energy.

In addition to dPT spectroscopy, we applied IR-R2PI spectroscopy^{11,16–18} to the PhOH(NH₃)₂ cluster. The NH-stretching vibrations are excited by using a tunable IR laser. The depopulation of the S_0 state is detected via a one- or two-color R2PI process.

II. EXPERIMENT

The R2PI measurements were performed with an apparatus described elsewhere.^{19,20} In short they were carried out using the frequency-doubled output of a Nd:YAG (Spectra Physics, GCR170) pumped dye laser (LAS, LDL205). The apparatus used for R2PI consists of a source chamber pumped with a 1000 l/s oil diffusion pump (Alcatel) in which the molecular beam is formed by expanding a mixture of helium, phenol, and ammonia through the 300 μm orifice of a pulsed nozzle (General Valve, Iota One). The skimmed molecular beam (Beam Dynamics Skimmer, 1 mm orifice) crosses the laser beams at right angles in the ionization chamber. The ions are extracted in a gridless Wiley–McLaren type time-of-flight (TOF) spectrometer perpendicular to the molecular beam and laser direction and enter the

^{a)}Authors to whom all correspondence should be addressed.

^{b)}Electronic mail: mschmitt@uni-duesseldorf.de

^{c)}Present address: University of Leeds, School of Chemistry, Leeds LS2 9JT, UK.

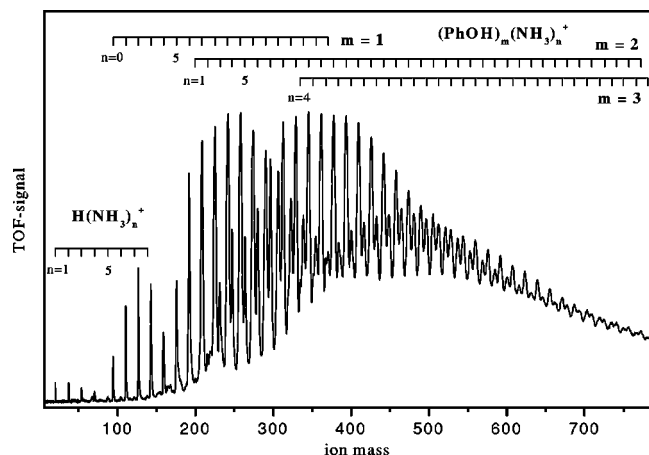


FIG. 1. Time-of-flight mass spectrum obtained by nonresonant multiphoton ionization of PhOH/NH₃ ($\lambda = 285$ nm). In addition to the PhOH_{*m*}(NH₃)_{*n*}⁺ cluster ions, fragment ions (NH₃)_{*n*}H⁺ can be observed.

drift chamber, where they are detected using multichannel plates (Galileo). Ionization and drift chamber are both pumped with a 150 l/s rotatory pump.

The apparatus to perform IR-R2PI double-resonance spectroscopy is described in Ref. 21. It consists of a differentially pumped linear TOF mass spectrometer and a pulsed valve (General Valve Iota One, 500 μ m orifice) for skimmed jet expansion ($X/D = 130$). Two frequency-doubled dye laser (Lumonics HD 300), each pumped by a Nd-YAG laser (Lumonics HY 400 and HY 750), were used to obtain a two color R2PI spectrum. The IR light (2.9–3.2 μ m) was generated with a LiNbO₃ crystal by difference frequency mixing of the fundamental (1064 nm) of a seeded Nd-YAG laser (Spectra-Physics GCR 3) and the output of a dye laser (LAS) pumped by the second harmonic (532 nm) of the same Nd-YAG laser. In order to produce a narrow distribution of phenol–ammonia clusters, phenol at room temperature was seeded into a mixture of helium and NH₃ and expanded through a pulsed nozzle at a stagnation pressure of 1 bar. For the PhOH(NH₃)_{*n*} clusters with $n < 10$ the best results were achieved with total ammonia concentrations of ≈ 0.25 vol %.

III. RESULTS AND DISCUSSION

Figure 1 shows a time-of-flight mass spectrum of a jet-cooled mixture of phenol and ammonia recorded after nonresonant two photon ionization at 285 nm. The ion signals on the mass channels of 1–3 phenol molecules with 0–35 ammonia molecules were recorded. Signals on the mass channels of the fragment ions (NH₃)_{*n*}H⁺ with $n = 1$ –8 could also be observed. The mass signals of these fragments are narrow ($\Delta m = 0.2 \equiv \Delta t = 36$ ns), while the mass signals of the PhOH(NH₃)_{*n*}⁺ cluster ions are broadened due to fragmentation in the acceleration region of the TOF. The sharp features of the fragment ions (NH₃)_{*n*}H⁺ lead to the conclusion that the fragmentation step which generates them is very rapid. The broader cluster ion peaks can be interpreted by a competing (slower) fragmentation channel, which may be attributed to the evaporation of (neutral) ammonia clusters from the cluster ion. For larger clusters, this

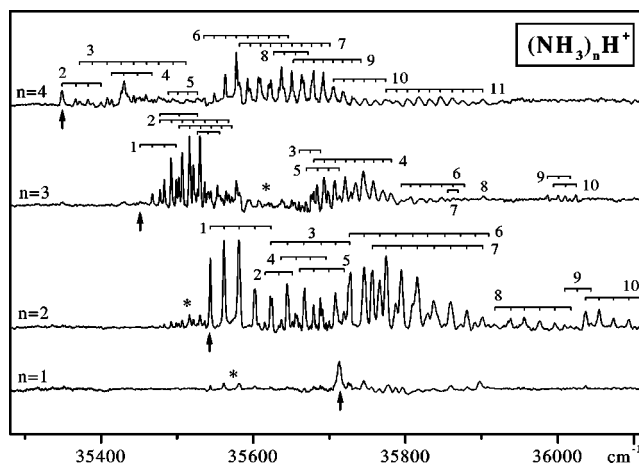


FIG. 2. R2PI spectra recorded on the mass channels of the (NH₃)_{*n*}H⁺ fragments. The corresponding cluster spectra (not given here) do not show any resonant signals on the mass channels of PhOH(NH₃)_{3,4}. The electronic origins are marked by arrows. Bands marked by an asterisk are due to fragmentation of the cluster with $n + 1$.

evaporation is considerably slower than for the smaller ones, causing the broadening of the mass signals in the TOF spectrum at higher masses (times).

The R2PI spectra recorded on the mass channels of PhOH(NH₃)_{*n*} show narrow bands under one-color conditions only for $n = 1$ and 2.²² Fragmentation of the $n = 2$ cluster can be reduced efficiently by two-color R2PI, but the resulting spectrum has a poor signal/noise ratio. Nevertheless, some vibronic bands could be assigned to the $n = 2$ cluster by this method. For clusters with $n \geq 2$, no resonance's could be unambiguously identified yet by two color R2PI measurements.

A. R2PI and dPT spectroscopy

Although nearly no resonant signal could be observed for the clusters with $n = 2$ –4 at the mass channel of the cluster ion, high quality resonant spectra of these clusters sizes were obtained by recording the R2PI signals at the (NH₃)_{*n*}H⁺ mass channel. The observed electronic origins of the phenol–ammonia clusters are indicated by arrows in Fig. 2. They are listed in Table I together with the spectral shifts relative to the phenol origin and the approximate excess energies in the ionic states after one-color excitation. We assigned the lowest energy transition, which is definitely not due to fragmentation, as the electronic origin, but we cannot

TABLE I. Electronic origins, spectral shifts, and excess energies in the D_0 states of the PhOH(NH₃)_{1–4} clusters. The spectral shifts are relative to the electronic origin of the phenol monomer at 36 348.7 cm^{-1} .

Cluster	Electronic origin (cm^{-1})	Spectral shift (cm^{-1})	D_0 excess energy ^a (cm^{-1})
PhOH(NH ₃) ₁	35 714.0	−634.7	8 100
PhOH(NH ₃) ₂	35 544.3	−804.4	9 100
PhOH(NH ₃) ₃	35 452.3	−896.4	10 300
PhOH(NH ₃) ₄	35 349.5	−999.2	15 100

^aThe ionization thresholds are taken from Ref. 2.

TABLE II. S_1 vibrational frequencies (cm⁻¹) of the $n=2$ cluster obtained by one-color R2PI. The bands were observed on the mass channel of the corresponding fragment ion (NH₃)₂H⁺.

Rel. position	Assignment	Rel. position	Assignment	Rel. position	Assignment
18.0	ν_1	164.5	$\nu_3 + 4\nu_1$	347.6	$\nu_6 + 8\nu_1$
37.4	$2\nu_1$	175.6	$\nu_5 + 3\nu_1$	357.7	$\nu_7 + 7\nu_1$
57.4/59.2	$3\nu_1$	182.0/184.4	$\nu_6/\nu_3 + 3\nu_1$	365.6	$\nu_6 + 9\nu_1$
71.7	ν_2	202.2	$\nu_6 + \nu_1$	373.8	ν_8
78.6/81.0	$4\nu_1/\nu_3$	212.9	ν_7	394.9	$\nu_8 + \nu_1$
89.9	$\nu_2 + \nu_1$	222.7	$\nu_6 + 2\nu_1$	412.9	$\nu_8 + 2\nu_1$
93.4	ν_4	231.2	$\nu_7 + \nu_1$	432.8	$\nu_8 + 3\nu_1$
100.5/102.1	$\nu_3 + \nu_1$	243.6	$\nu_6 + 3\nu_1$	453.0	$\nu_8 + 4\nu_1$
108.0	$\nu_2 + 2\nu_1$	251.1	$\nu_7 + 2\nu_1$	465.7	ν_9
111.9/114.1	$\nu_4 + \nu_1$	265.9	$\nu_6 + 4\nu_1$	473.5	$\nu_8 + 5\nu_1$
117.6	ν_5	272.0	$\nu_7 + 3\nu_1$	481.1/483.9	$\nu_9 + \nu_1$
122.1/124.1	$\nu_3 + 2\nu_1$	285.8	$\nu_6 + 5\nu_1$	493.3	ν_{10}
130.6/131.9	$\nu_4 + 2\nu_1$	293.8	$\nu_7 + 4\nu_1$	500.3	$\nu_9 + 2\nu_1$
135.7	$\nu_5 + \nu_1$	307.7	$\nu_6 + 6\nu_1$	510.9	$\nu_{10} + \nu_1$
144.5/147.0	$\nu_3 + 3\nu_1$	315.8	$\nu_7 + 5\nu_1$	529.8	$\nu_{10} + 2\nu_1$
152.3	$\nu_4 + 3\nu_1$	329.4	$\nu_6 + 7\nu_1$	550.1	$\nu_{10} + 3\nu_1$
155.6	$\nu_5 + 2\nu_1$	337.3	$\nu_7 + 6\nu_1$	571.3	$\nu_{10} + 4\nu_1$

exclude that an unfavorable Franck–Condon pattern of the long progressions shown in Fig. 2 prevents the observation of the true origin.

The dPT spectra of PhOH(NH₃)_{2,3} in Fig. 2 show quite long harmonic progressions of low frequency vibrations ν_1 at 18 ($n=2$) and 16 cm⁻¹ ($n=3$). Obviously, there is a considerable change in geometry along the corresponding normal coordinate after electronic excitation.

The spectrum observed at the $n=4$ mass trace shows progressions with two low frequency vibrations. One progression with 18 cm⁻¹ spacing (ν_2 in Table IV) is based upon the electronic origin and upon other intermolecular vibrations, while the second progression with 13 cm⁻¹ spacing (ν_1 in Table IV) can only be observed in combination with other vibrations. It cannot be excluded that the spectrum with the 13 cm⁻¹ progressions belongs to another isomer of PhOH(NH₃)₄ or is due to fragmentation of a higher cluster. Very little fragmentation is observed on the mass channels of

the $n=1, 2, 3$ clusters, which probably arises from the consumption of most of the ion excess energy by separation of the phenoxy radical. Therefore we consider it to be unlikely that the 13 cm⁻¹ progression observed at the $n=4$ mass channel arises from higher clusters. Future SHB experiments will clarify if the second progression is due to another conformer of the $n=4$ cluster. The S_1 vibrational frequencies of the $n=2-4$ clusters are summarized in Tables II–IV.

In the following we will discuss the $n=2$ cluster spectrum shown in Fig. 2 in greater detail. Redshifted to the electronic origin at 35 544.3 cm⁻¹ are some weak bands, which coincide with intense bands of the $n=3$ cluster and can be attributed to its fragmentation. The remaining signals can be assigned to the $n=2$ cluster and are listed in Table II.

The lowest frequency vibration at 18 cm⁻¹ is observed as a long progression in combination with most of the other vibrations. Figure 3 shows the two-color R2PI spectrum of PhOH(NH₃)₂ in the region of the $0_0^0 + n\nu_1$ progression in

TABLE III. S_1 vibrational frequencies (cm⁻¹) of the $n=3$ cluster obtained by one-color R2PI. The bands were observed on the mass channel of the corresponding fragment ion (NH₃)₃H⁺.

Rel. position	Assignment	Rel. position	Assignment	Rel. position	Assignment
15.9	ν_1	116.4	$\nu_2 + 6\nu_1$	329.8	$\nu_5 + 8\nu_1$
26.0	ν_2	120.4	$2\nu_2 + 5\nu_1$	343.1	ν_6
31.8	$2\nu_1$	208.7	ν_3	355.4	$\nu_6 + \nu_1$
40.6	$\nu_2 + \nu_1$	218.0	ν_4	367.8	$\nu_6 + 2\nu_1$
47.3	$4\nu_1/\nu_3$	224.4	$\nu_3 + \nu_1$	381.5	$\nu_6 + 3\nu_1$
50.7	$2\nu_2$	227.8	ν_5	396.3	$\nu_6 + 4\nu_1$
55.1	$\nu_2 + 2\nu_1$	232.5	$\nu_4 + \nu_1$	403.9	ν_7
64.8	$2\nu_2 + \nu_1$	237.1	$\nu_3 + 2\nu_1$	411.4	$\nu_6 + 5\nu_1$
69.8	$\nu_2 + 3\nu_1$	241.8	$\nu_5 + \nu_1$	418.0	$\nu_7 + \nu_1$
75.3	$3\nu_2$	246.9	$\nu_4 + 2\nu_1$	426.7	$\nu_6 + 6\nu_1$
78.6	$2\nu_2 + 2\nu_1$	255.6	$\nu_5 + 2\nu_1$	451.6	ν_8
84.8	$\nu_2 + 4\nu_1$	260.3/261.9	$\nu_5 + 3\nu_1$	535.3	ν_9
88.1/89.5	$3\nu_2 + \nu_1$	269.5	$\nu_7 + 4\nu_1$	541.6	ν_{10}
92.6	$2\nu_2 + 3\nu_1$	278.7/282.2	$\nu_5 + 4\nu_1$	549.7	$\nu_9 + \nu_1$
101.4	$\nu_2 + 5\nu_1$	293.4	$\nu_5 + 5\nu_1$	558.8	$\nu_{10} + \nu_1$
103.8/105.2	$3\nu_2 + 2\nu_1$	306.3	$\nu_5 + 6\nu_1$	564.7	$\nu_9 + 2\nu_1$
108.0	$2\nu_2 + 4\nu_1$	319.1	$\nu_5 + 7\nu_1$	572.6	$\nu_{10} + 2\nu_1$

TABLE IV. S_1 vibrational frequencies (cm^{-1}) of the $n=4$ cluster obtained by one-color R2PI. The bands were observed on the mass channel of the corresponding fragment ion $(\text{NH}_3)_4\text{H}^+$.

Rel. position	Assignment	Rel. position	Assignment	Rel. position	Assignment
17.7	ν_2	185.5	ν_6	340.5	$\nu_7 + 8\nu_1$
23.2	ν_3	187.6		343.3	$\nu_9 + 3\nu_1$
33.9	$2\nu_2$	193.5		351.8	$\nu_7 + 9\nu_1$
40.0	$\nu_3 + \nu_2$	200.3	$\nu_6 + \nu_1$	355.7	$\nu_9 + 4\nu_1$
51.0	$3\nu_2$	214.6	$\nu_6 + 2\nu_1$	357.3	ν_{10}
59.3	$\nu_3 + 2\nu_2$	229.2	$\nu_6 + 3\nu_1$	369.3	$\nu_9 + 5\nu_1$
65.3	ν_4	232.9	ν_7	371.6	$\nu_{10} + \nu_1$
78.0	$\nu_3 + 3\nu_2$	243.8	$\nu_6 + 4\nu_1$	381.3	$\nu_9 + 6\nu_1$
81.6	$\nu_4 + \nu_2$	246.9	$\nu_7 + \nu_1$	383.0	$\nu_{10} + 2\nu_1$
85.2		258.2	$\nu_6 + 5\nu_1$	392.9	$\nu_9 + 7\nu_1$
87.8		260.6	$\nu_7 + 2\nu_1$	397.3	$\nu_{10} + 3\nu_1$
94.2	$\nu_3 + 4\nu_2$	271.8	$\nu_6 + 6\nu_1$	398.8	
98.6	$\nu_4 + 2\nu_2$	274.4	$\nu_7 + 3\nu_1$	412.0	$\nu_{10} + 4\nu_1$
102.0		278.4	ν_8	424.8	$\nu_{10} + 5\nu_1$
106.2		285.0	$\nu_6 + 7\nu_1$	427.0	ν_{11}
110.5	$\nu_3 + 5\nu_2$	288.5	$\nu_7 + 4\nu_1$	430.1	
117.8	$\nu_4 + 3\nu_2$	291.6	$\nu_8 + \nu_1$	440.3	$\nu_{11} + \nu_1$
121.6		297.4	$\nu_6 + 8\nu_1$	454.0	$\nu_{11} + 2\nu_1$
127.0	$\nu_3 + 6\nu_2$	301.9	$\nu_7 + 5\nu_1$	468.7	$\nu_{11} + 3\nu_1$
130.1		304.5	ν_9	483.2	$\nu_{11} + 4\nu_1$
133.9		306.5	$\nu_8 + 2\nu_1$	497.7	$\nu_{11} + 5\nu_1$
139.7	ν_5	312.6		512.7	$\nu_{11} + 6\nu_1$
146.1	$\nu_3 + 7\nu_2$	315.2	$\nu_7 + 6\nu_1$	527.1	$\nu_{11} + 7\nu_1$
152.2	$\nu_5 + \nu_1$	317.4	$\nu_9 + \nu_1$	539.6	$\nu_{11} + 8\nu_1$
163.4	$\nu_3 + 8\nu_2$	323.3	$\nu_8 + 3\nu_1$	553.1	$\nu_{11} + 9\nu_1$
165.4	$\nu_5 + 2\nu_1$	327.5	$\nu_7 + 7\nu_1$		
178.1	$\nu_5 + 3\nu_1$	330.5	$\nu_9 + 2\nu_1$		

more detail. Each band is split into two components whose spacing increases with increasing energy, indicating the existence of a tunneling motion or different conformers. In principle the splitting can also arise from a hot band contribution. This can be excluded, however, because the intensity ratio of the splitted bands does not depend on the expansion conditions.

B. IR-R2PI spectroscopy

Before considering any large amplitude motion, which may lead to energetically equivalent conformers of $\text{PhOH}(\text{NH}_3)_2$ and thus to the observed splitting of the spectrum, more information about the geometry of the $n=2$ cluster has to be obtained. Therefore the IR-R2PI spectrum of $\text{PhOH}(\text{NH}_3)_2$ has been taken in the range of the $-\text{OH}$ and $-\text{NH}$ stretching vibration. The spectrum has been recorded in the range from 3150 to 3450 cm^{-1} (cf. Fig. 4). The depopulation of the ground state has been detected via the two-color R2PI signal at the electronic origin of the $\text{PhOH}(\text{NH}_3)_2$ cluster.

The excitation laser was fixed to 35 544.3 cm^{-1} , which is the low frequency component of the splitted electronic origin. The ionization laser was fixed to 28 571 cm^{-1} (350 nm), which is slightly above the ionization potential to reduce the amount of fragmentation. Unfortunately, the splitting of the origin is too small to obtain IR-R2PI spectra of both components.

C. Calculations

In order to interpret the infrared spectra, Hartree-Fock [6-31G, 6-31G(*d*), and 6-31G(*d,p*) basis sets] and second-order Møller-Plesset calculations [6-31G(*d*) basis set] have been performed using the GAUSSIAN 98 program package.²³ From all calculations it can be concluded that there are two minimum energy structures which have nearly the same energy if zero point energy (ZPE) corrections and the basis set superposition error (BSSE) using the counterpoise procedure of Boys and Bernardi²⁴ are taken into account. The first structure is a cyclic arrangement of phenol and the two ammonia molecules [cf. Fig. 5 (b)]. In this structure the ammonia molecule (1) forms a nearly linear hydrogen bond with the phenolic hydroxyl group, while the other NH_3 molecule forms hydrogen bonds to NH_3 (1) and to phenol, which therefore acts as proton donor and acceptor. The total binding energy calculated for this structure at the MP2/6-31G(*d*) level of theory including ZPE and BSSE is 4350 cm^{-1} (52.1 kJ/mol). Since there are three hydrogen bonds in this structure an average binding energy of 1450 cm^{-1} (17.4 kJ/mol) per hydrogen bond is obtained.

The second structure of $\text{PhOH}(\text{NH}_3)_2$ [cf. Fig. 5 (a)] is an open arrangement. This configuration is stabilized by an interaction of an ammonia (2) H atom with the aromatic π system. The total binding energy of this structure is 4381 cm^{-1} (52.4 kJ/mol), obtained at the MP2/6-31G(*d*) level of theory including ZPE and BSSE. Since the calculated energy difference between the cyclic and open structure is less than 100 cm^{-1} , no reliable information about the relative energies

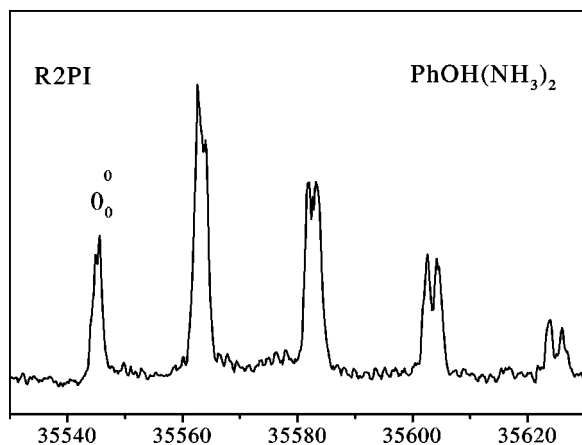


FIG. 3. Two-color R2PI spectrum of the ν_1 progression in the region of the electronic origin of PhOH(NH₃)₂, recorded at the mass channel of PhOH(NH₃)₁. Every transition is also observed on the mass channel of PhOH(NH₃)₂ but with a somewhat worse signal-to-noise ratio. The ionization laser was held fixed at 355 nm.

of both structures can be obtained from calculations applying basis sets of double-zeta quality.

A structural assignment may be obtained by comparing the calculated and experimentally observed frequencies of the intramolecular OH- and NH-stretching vibrations. To obtain the OH- and NH-stretching frequencies of the cyclic and open PhOH(NH₃)₂ clusters normal vibrational analyses of both structures have been carried out at the HF and MP2 level. The scaled vibrational frequencies obtained from the MP2 [6-31G(*d*) basis] calculations are given in Table V.

In all calculations performed at the HF level the symmetric and antisymmetric NH-stretching vibrations (see Table V) exhibit only small changes with respect to the different basis sets. In contrast to this, the OH-stretching frequency shows a large difference by changing the basis set. In the case of the 6-31G(*d,p*) basis the OH-stretching motion turns out to be the vibration with the highest frequency. For

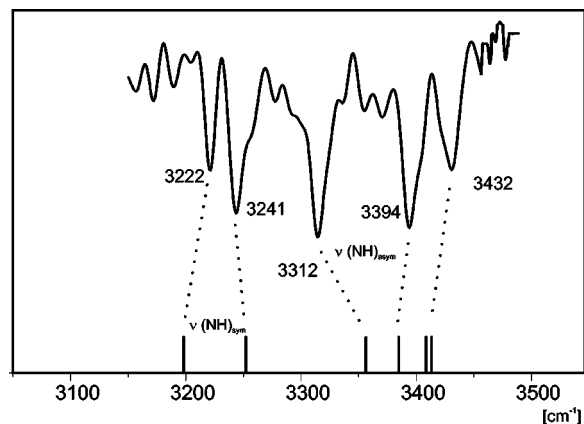


FIG. 4. The IR-R2PI spectrum of PhOH(NH₃)₂ shown in the range from 3150 to 3450 cm⁻¹. The transitions can be assigned to the symmetric and antisymmetric NH-stretching vibrations of the ammonia molecules (see Table V). The antisymmetric stretching vibrations are either more localized on the bound N-H bonds (3312 and 3394 cm⁻¹) or the free N-H bonds (3432 cm⁻¹). At the bottom the calculated scaled frequencies obtained for the cyclic structure are given.

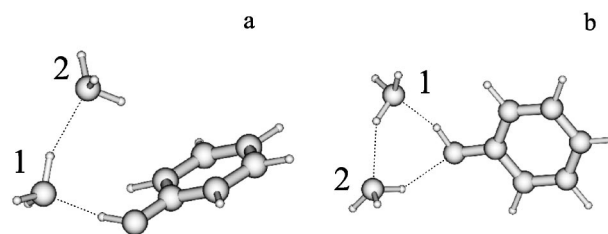


FIG. 5. The open and cyclic structures of PhOH(NH₃)₂ as obtained from the MP2/6-31G(*d*) calculations. In the cyclic structure two H atoms of the ammonia molecules undergo a hydrogen bond, whereas the remaining H atoms of the ammonia molecules belong to the free NH groups. The open structure is stabilized by an interaction between NH₃(2) and the π system of the aromatic ring.

the 6-31G(*d*) basis the frequency of the OH-stretching mode is between the symmetric and antisymmetric NH-stretching vibrations. In the case of the 6-31G basis the OH-stretching frequency is lower than all NH-stretching modes. By applying the MP2 method [6-31G(*d*) basis] the calculated frequency of the OH-stretching vibration is shifted below the CH-stretching modes. For an interpretation of the IR-R2PI spectra not only the calculated frequencies but also the intensities have to be taken into account. According to all calculations the intensity of the OH-stretching modes should be much larger than the intensity of the NH-stretching modes. The comparable intensity of all vibrations obtained in the IR-R2PI spectra indicate that only NH-stretching vibrations are observed. This result is in agreement with the IR-R2PI spectra of 1-naphthol(NH₃)₂.²⁵ The OH-stretching frequency of this cluster is observed as a very broad transition at 3100 cm⁻¹. An assignment of the NH-stretching vibrations is given in Table V. This assignment is in agreement with all calculations performed at the HF and MP2 level.

Although all vibrations in the IR-R2PI spectrum of PhOH(NH₃)₂ can be assigned, no structural information with respect to a cyclic or open arrangement of this cluster can be obtained since the calculated frequencies for both structures are nearly identical. The following consideration gives a hint as to whether a cyclic or an open arrangement is the most stable one: The cyclic structure of PhOH(NH₃)₂ is similar to the PhOH(H₂O)₂ geometry.^{26,27} However, the R2PI spectra of these species are very different. The broad bands

TABLE V. Experimentally observed and calculated NH-stretching frequencies of the cyclic and open PhOH(NH₃)₂ cluster. The calculated frequencies are obtained from the MP2 calculations [6-31G(*d,p*) basis] and scaled by a factor of 0.93. The scaled frequencies obtained from HF calculations [6-31G, 6-31G(*d*), 6-31G(*d,p*) basis] are similar to the frequencies obtained at the MP2 level. The vibrations can be assigned with respect to symmetric and antisymmetric vibrations of the NH₃ moieties (see Figs. 5 and 4).

NH-stretching frequencies			
Cyclic structure	Open structure	Experimental	Assignment
3198	3185	3222	sym. NH ₃ (1)
3253	3259	3241	sym. NH ₃ (2)
3358	3351	3312	asym. NH ₃ (1), bound
3386	3394	3394	asym. NH ₃ (2), bound
3410	3406		asym. NH ₃ (2), free
3415	3415	3432	asym. NH ₃ (1), free

in the $\text{PhOH}(\text{H}_2\text{O})_2$ spectrum can be traced back to an opening of the H-bridged ring at the phenol acceptor position upon electronic excitation.²⁶ The narrow bands in the $\text{PhOH}(\text{NH}_3)_2$ cluster spectrum (cf. Fig. 2) point to a stable structure in the S_1 state. This may be attributed to the higher electron density at the phenolic O atom due to the higher basicity of ammonia compared to water preserving a cyclic arrangement in the S_1 state.

A normal mode analysis based on the cyclic geometry optimized at the HF/6-31G(*d,p*) and MP2/6-31G(*d*) level for the intermolecular modes leads to 13 and 18 cm^{-1} , respectively, as lowest frequency vibration (ν_1). This mode can be described by a butterfly motion of the two rings, which is very similar to the lowest frequency modes of the cyclic phenol–water clusters $\text{PhOH}(\text{H}_2\text{O})_{2-4}$.²⁷ In the cyclic structure one of the two ammonia moieties, i.e., its center of mass, nearly lies in the aromatic plane [in Fig. 5(b)], whereas the other one (2) is located a considerable distance from this plane. A large amplitude butterfly motion can lead to a geometry in which the ammonia molecule 2 changes its position from one side of the C–O–N(1) plane to the other side, resulting in an energetically equivalent enantiomeric structure. If the equilibrium geometry along the butterfly motion (ν_1) changes in the S_1 state, Franck–Condon factors can lead to a long vibrational progression in the R2PI spectrum. Assuming a ν_1 tunneling motion, $\text{PhOH}(\text{NH}_3)_2$ can be classified in the molecular symmetry group G_2 with the operations E and P^* .²⁸ The permutation inversion operation P^* is composed of the spatial inversion at the center of mass and the permutation of two protons in both ammonia moieties to conserve their handedness. The resulting spin statistical weights of the two lowest energy levels agree with the experimental intensities, which are 1:1 for the two torsional components. We tried to fit the progression of the ν_1 mode by the method of Lewis *et al.*²⁹ using V_1 , V_2 , and V_4 barriers. The results of these calculations are not physically satisfying, pointing to either a tunneling motion, which cannot be described by a one-dimensional approximation, or the existence of two different isomers of $\text{PhOH}(\text{NH}_3)_2$. If we assume that the open structure is correct, it is suggestive that the tunneling motion is the threefold rotation about the symmetry axis of ammonia molecule 2. Again, the spin statistical weight is 1:1. The larger splitting of the torsional components compared to the 1:1 complex could be traced back to a greater difference between the S_0 and S_1 barriers caused by the different π interaction with the rotating ammonia moiety.

Although there is a change of the vibrational frequencies between the S_0 and S_1 states the intermolecular stretching vibrations obtained from the *ab initio* calculations of the S_0 state can be taken as an approximation to interpret the three prominent vibrations ν_5 (117.6 cm^{-1}), ν_6 (182.1 cm^{-1}), and ν_7 (212.9 cm^{-1}) of the R2PI spectrum. Each of the stretching vibrations forms progressions with the ν_1 vibration (cf. Table II and Fig. 2). The ν_7 vibration (calculated: cyclic structure: 217 cm^{-1} , open structure: 209 cm^{-1}) corresponds to the stretching vibration between phenol and ammonia (1). The ν_6 vibration can be assigned as the stretching vibration between the two ammonia molecules (calculated: cyclic structure: 188 cm^{-1} , open structure: 186 cm^{-1}),

whereas the ν_5 vibration can be interpreted as stretching vibration between phenol and ammonia (2) (calculated: cyclic structure: 116 cm^{-1}) or as stretching vibration between ammonia (2) and the π system of phenol (calculated: open structure: 108 cm^{-1}).

The S_1 spectrum of $\text{PhOH}(\text{NH}_3)_3$ is similar to the $n=2$ cluster spectrum and some bands are split as well. Hence, the structure should be similar to that of $\text{PhOH}(\text{NH}_3)_2$, in agreement with the *ab initio* calculations predicting a cyclic geometry.¹⁰ The calculated lowest frequency mode is again the butterfly motion with an S_0 value of 6.9 cm^{-1} . The large difference to the calculated ν_1 frequency of the $n=2$ cluster (13.3 cm^{-1}) is not found experimentally. The experimental lowest frequency mode, which forms long progressions, has a frequency of 16 cm^{-1} . The S_1 vibrational frequencies are summarized in Table III.

Ab initio calculations at the HF/6-31G(*d*) level point to an $n=4$ cluster structure with a cyclic $\text{PhOH}(\text{NH}_3)_3$ moiety and the fourth ammonia lying on one side of the aromatic ring.¹⁰ The interaction with the aromatic π system should have a greater influence on the spectral shift compared to the $n=3$ electronic origin. Since the spectral shift between the origins of the $n=2$ and $n=3$ clusters is very similar to that between the clusters with $n=3$ and $n=4$, we assume the geometry of the $\text{PhOH}(\text{NH}_3)_4$ cluster to be cyclic as well. It should be mentioned that relative stabilities obtained from HF calculations using double-zeta basis sets are always questionable, since the level of the method and the size of the basis set is too low. The Hartree–Fock calculations can only indicate different possibilities, if several structures of similar energy have to be taken into account.

For the $\text{PhOH}(\text{NH}_3)_4$ cluster no splitting could be observed. In contrast to the clusters with $n=2$ and 3, progressions of two low frequency modes of 13 and 18 cm^{-1} are present in the dPT spectrum. Assuming a cyclic structure these could be the butterfly and the twisting modes of the two moieties (calculated frequencies: 8.3/14.7 cm^{-1}). The third mode, which can be described by a mutual rotation about the c axis of phenol and the corresponding axis of the other moiety, has a distinctly higher frequency (32.1 cm^{-1}). The experimental band positions are summarized in Table IV.

For the interested reader the vibrations and different structural arrangements of the $\text{PhOH}(\text{NH}_3)_n$ clusters can be obtained via the internet address <http://www-public.rz.uni-duesseldorf.de/~pc1/abinitio/index.html> and animated with programs like MOLGEN or XMOL.

IV. CONCLUSIONS

dPT spectroscopy could be shown to be an interesting tool to obtain information about the vibronic structure of small phenol–ammonia clusters. *Ab initio* calculations of the S_0 harmonic frequencies can only give tendencies and do not efficiently support the vibrational assignments in the S_1 state. There are some arguments that the $\text{PhOH}(\text{NH}_3)_{2-4}$ clusters have cyclic structures, which are similar to the corresponding phenol–water clusters, but an open structure of $\text{PhOH}(\text{NH}_3)_2$ cannot be excluded from IR-R2PI spectroscopy and *ab initio* calculations. Nevertheless, the spectra of

phenol–ammonia and phenol–water clusters are considerably different. This can be attributed to the distinct acid-base character in the phenol–ammonia clusters.

ACKNOWLEDGMENT

We gratefully acknowledge the financial support of the Deutsche Forschungsgemeinschaft (Schwerpunkt "Molekulare Cluster").

- ¹N. Mikami, A. Okabe, and I. Suzuki, *J. Phys. Chem.* **92**, 1858 (1988).
- ²D. Solgadi, C. Jouvet, and A. Tramer, *J. Phys. Chem.* **92**, 3313 (1988).
- ³C. Jouvet, C. Lardeux-Dedonder, M. Richard-Viard, D. Solgadi, and A. Tramer, *J. Phys. Chem.* **94**, 5041 (1990).
- ⁴A. Crepin and A. Tramer, *Chem. Phys.* **156**, 281 (1991).
- ⁵J. A. Syage and J. Steadman, *J. Phys. Chem.* **96**, 9606 (1992).
- ⁶A. Schiefke, C. Deussen, C. Jacoby, M. Gerhards, M. Schmitt, K. Kleinermanns, and P. Hering, *J. Chem. Phys.* **102**, 9197 (1995).
- ⁷J. A. Syage, in *Femtosecond Chemistry*, edited by J. Manz and L. Wöste (Chemie, Berlin, 1995).
- ⁸A. Iwasaki, A. Fujii, T. Watanabe, T. Ebata, and N. Mikami, *J. Phys. Chem.* **100**, 16053 (1996).
- ⁹M. Yi and S. Schreiner, *Chem. Phys. Lett.* **262**, 567 (1996).
- ¹⁰W. Siebrand, M. Z. Zgierski, Z. K. Smedarchina, M. Vener, and J. Kaneti, *Chem. Phys. Lett.* **266**, 47 (1997).
- ¹¹B. Brutschy, *Chem. Rev.* **92**, 1567 (1992).
- ¹²N. Mikami, S. Sato, and M. Ishigaki, *Chem. Phys. Lett.* **202**, 431 (1993).
- ¹³H. T. Kim, R. J. Green, J. Qian, and S. L. Anderson, *J. Chem. Phys.* **112**, 5717 (2000).
- ¹⁴K. Fuke, R. Takasu, and F. Misaizu, *Chem. Phys. Lett.* **229**, 597 (1994).
- ¹⁵G. A. Pino, C. Dedonder-Lardeux, G. Grégoire, C. Jouvet, S. Martrenchard, and D. Solgadi, *J. Chem. Phys.* **111**, 10747 (1999).
- ¹⁶S. Djafari, H.-D. Barth, K. Buchhold, and B. Brutschy, *J. Chem. Phys.* **107**, 10573 (1997).
- ¹⁷T. Ebata, A. Fujii, and N. Mikami, *Int. J. Mass Spectrom. Ion Processes* **159**, 111 (1996).
- ¹⁸F. C. Hagemester, C. J. Gruenloh, and T. S. Zwier, *J. Phys. Chem.* **102**, 82 (1998).
- ¹⁹M. Schmitt, C. Jacoby, and K. Kleinermanns, *J. Chem. Phys.* **108**, 4486 (1998).
- ²⁰W. Roth, C. Jacoby, A. Westphal, and M. Schmitt, *J. Phys. Chem. A* **102**, 3048 (1998).
- ²¹M. Gerhards, M. Schiwek, C. Unterberg, and K. Kleinermanns, *Chem. Phys. Lett.* **297**, 515 (1996).
- ²²C. Jacoby, P. Hering, M. Schmitt, W. Roth, and K. Kleinermanns, *Chem. Phys.* **239**, 23 (1998).
- ²³M. J. Frisch, G. W. Trucks, H. B. Schlegel, G. E. Scuseria, M. A. Robb, J. R. Cheeseman, V. G. Zakrzewski, J. A. Montgomery, Jr., R. E. Stratmann, J. C. Burant, S. Dapprich, J. M. Millam, A. D. Daniels, K. N. Kudin, M. C. Strain, O. Farkas, J. Tomasi, V. Barone, M. Cossi, R. Cammi, B. Mennucci, C. Pomelli, C. Adamo, S. Clifford, J. Ochterski, G. A. Petersson, P. Y. Ayala, Q. Cui, K. Morokuma, D. K. Malick, A. D. Rabuck, K. Raghavachari, J. B. Foresman, J. Cioslowski, J. V. Ortiz, A. G. Baboul, B. B. Stefanov, G. Liu, A. Liashenko, P. Piskorz, I. Komaromi, R. Gomperts, R. L. Martin, D. J. Fox, T. Keith, M. A. Al-Laham, C. Y. Peng, A. Nanayakkara, C. Gonzalez, M. Challacombe, P. M. W. Gill, B. Johnson, W. Chen, M. W. Wong, J. L. Andres, C. Gonzalez, M. Head-Gordon, E. S. Replogle, and J. A. Pople, *GAUSSIAN 98*, Revision A.7, Gaussian, Inc., Pittsburgh, PA, 1998.
- ²⁴S. F. Boys and F. Bernardi, *Mol. Phys.* **19**, 553 (1970).
- ²⁵Y. Matsumoto, T. Ebata, and N. Mikami (unpublished).
- ²⁶M. Gerhards and K. Kleinermanns, *J. Chem. Phys.* **103**, 7392 (1995).
- ²⁷C. Jacoby, W. Roth, M. Schmitt, C. Janzen, D. Spangenberg, and K. Kleinermanns, *J. Phys. Chem. A* **102**, 4471 (1998).
- ²⁸H. C. Longuet-Higgins, *Mol. Phys.* **6**, 445 (1963).
- ²⁹J. D. Lewis, T. D. Malloy, T. H. Chao, and J. Laane, *J. Mol. Struct.* **12**, 427 (1972).